

AperTO - Archivio Istituzionale Open Access dell'Università di Torino

Biological and molecular characterization of *Chenopodium quinoa* mitovirus 1 reveals a distinct sRNA response compared to cytoplasmic RNA viruses.

This is the author's manuscript

Original Citation:

Availability:

This version is available <http://hdl.handle.net/2318/1694939> since 2019-03-18T09:03:49Z

Published version:

DOI:10.1128/JVI.01998-18

Terms of use:

Open Access

Anyone can freely access the full text of works made available as "Open Access". Works made available under a Creative Commons license can be used according to the terms and conditions of said license. Use of all other works requires consent of the right holder (author or publisher) if not exempted from copyright protection by the applicable law.

(Article begins on next page)

This is the author's final version of the contribution published as:

[L. Nerva, G. Vigani, D. Di Silvestre, M. Ciuffo, M. Forgia, W. Chitarra, M. Turina. Biological and molecular characterization of *Chenopodium quinoa* mitovirus 1 reveals a distinct sRNA response compared to cytoplasmic RNA viruses., *Journal of Virology*. In press DOI: 10.1128/JVI.01998-18]

The publisher's version is available at:

[inserire URL sito editoriale presa dal campo URL, cioè dc.identifier.url]

When citing, please refer to the published version.

Link to this full text:

[inserire l'handle completa, preceduta da

<https://jvi.asm.org/content/early/2019/01/10/JVI.01998-18.long>]

ABSTRACT

Indirect evidence of mitochondrial viruses in plants comes from discovery of genomic fragments integrated into the nuclear and mitochondrial DNA of a number of plant species. Here, we report the existence of replicating mitochondrial virus in plants: from RNAseq data of infected *Chenopodium quinoa*, a plant species commonly used as a test plant in virus host-range experiments, among other virus contigs, we could assemble a 2.7 Kb contig that had highest similarity to mitoviruses found in plant genomes. Northern blot analyses confirmed the existence of plus and minus strand RNA corresponding to the mitovirus genome. No DNA corresponding to the genomic RNA was detected, excluding the endogenization of such virus. We have tested a number of *C. quinoa* accessions, and the virus was present in a number of commercial varieties, but absent from a large collection of Bolivian and Peruvian accessions. The virus could not be transmitted mechanically or by grafting, but it is transmitted vertically through seeds at a 100% rate. Small RNA analysis of a *C. quinoa* line carrying the mitovirus and infected by alfalfa mosaic virus showed that the typical anti-viral silencing response active against cytoplasmic viruses (21-22 nt vsRNA peaks) is not active against CqMV1, since in this specific case the highest accumulating vsRNA length is 16, which is the same as that corresponding to RNA from mitochondrial genes. This is evidence of a distinct viral RNA degradation mechanism active inside mitochondria that could possibly have also an anti-viral effect.

IMPORTANCE

This paper reports the first biological characterization of a bona fide plant mitovirus in an important crop, *Chenopodium quinoa*, providing data supporting that mitoviruses have the typical features of cryptic (persistent) plant viruses. We for the first time demonstrate that plant mitoviruses are associated with mitochondria in plants. In contrast with fungal mitoviruses, plant mitoviruses are not substantially affected by the anti-viral silencing pathway, and the most abundant mitovirus small RNA length is 16 nt.

Copyright © 2019 American Society for Microbiology.

All Rights Reserved.

INTRODUCTION

The family *Narnaviridae* comprises two genera of positive single-stranded (ss) RNA viruses, 52 the *Narnavirus* and the *Mitovirus*, both originally thought to be mycoviruses, because fungi are the 53 main natural host in which they can replicate. Both are known to be naked viruses presenting only one 54 ORF that encodes one protein, the RNA-dependent RNA polymerase (RdRp) (1). The two genera are 55 distinguished based on phylogenetic analysis (each of them belongs to a distinct, statistically well-56 supported clade) and on subcellular localization: the narnaviruses replicate and stay in cytosol, 57 whereas the mitoviruses typically replicate and persist in the mitochondrion. Evidence of their 58 mitochondrial localization is provided by the fact that they fractionate with the mitochondrial fraction 59 (2) and that for most of them the ORF is translated using the mitochondrial genetic code (1). The 60 mitoviruses described so far are able to infect only mitochondria of filamentous fungi and in some 61 cases they are associated with hypovirulence (1). Sometimes it seems that the mitochondrial 62 morphology is not affected by the virus, whereas in some other cases they can cause a morphological 63 alteration (i.e. fibrous mitochondria) which were possibly associated with the induced hypovirulence 64 (3). 65

Some fungal mitoviruses have the potential to use both the nuclear and mitochondrial genetic 66 code for the translation of their genomes, and based on this, some authors have hypothesized 67 promiscuous replication in both mitochondria and cytoplasm. However, bioinformatic analysis leads 68 to a different explanation: in those host species where mitovirus RdRp can hypothetically be translated 69 using both genetic codes, the mitochondrial genes have a strong bias for the tryptophan codon that is 70 shared with the nuclear genetic code (UGG). This implies that the exclusive use of UGG codon for 71

tryptophan in some mitovirus is not because of a promiscuous lifestyle between mitochondria and 72
cytoplasm, but it reflects the fact that UGA (the only differential codon between the nuclear and 73
on February 4, 2019 by guest<http://jvi.asm.org/>Downloaded from
Nerva et al. J. Virol.

mitochondrial genetic codes in the fungal-plant host species) is not present in general in genes 74
encoded by the mitochondria (4). 75

Intriguingly, species of genus Mitovirus are most closely related to the Leviviridae, the only 76
taxonomically defined group of (+)ssRNA bacterial phages (5, 6). Within the context of the theory of 77
mitochondria derived from an alpha-proteobacterial endosymbiont (7), this suggests that mitoviruses 78
likely derived from an ancestral mitochondrial phage by losing the capsid protein (CP) (8) which is 79
unnecessary due to the absence of an extracellular stage (9). 80

A further interesting observation related to mitoviruses comes from the availability of a great 81
number of complete plant and fungal genomes that were mined to reveal the presence of non-retroviral 82
endogenous RNA viral elements (NERVES): complete genomes or partial/complete gene sequences of 83
RNA viruses are present in almost all the eukaryotic nuclear genomes (10-13). Specifically, Bruenn 84
and co-authors demonstrated the widespread presence of mitoviral sequences in many plant nuclear 85
and mitochondrial genomes (13). Two different hypotheses can explain this evidence: the first is 86
diverse integration events of a fungal mitovirus, or of a native plant mitochondrial virus, into the 87
mitochondrial genome, and from here to the nucleus as a result of mitochondrial DNA transfer (13, 88
14); the second proposes the possibility of integration of such sequences in plant genomes via fungal 89
mediated horizontal gene transfer (HGT) during the long-term coevolution of fungi and plants (15, 90
16). Very recently, indirect evidence of replicating plant mitoviruses was provided mining the 91
transcriptome of a number of plant species (17). 92

We here report the complete genome sequence and biological characterization of a replicating 93
plant mitovirus detected in a number of *Chenopodium quinoa* accessions and designated as 94
Chenopodium quinoa mitovirus 1 (CqMV1). Furthermore, we provide evidence of differential small 95
RNA (sRNA) processing of this virus compared to a cytoplasmic plant virus infecting the same plant, 96
indicating the possible involvement of a still uncharacterized new differential anti-viral response 97
inside the mitochondria. 98

99

on February 4, 2019 by guest<http://jvi.asm.org/>Downloaded from
Nerva et al. J. Virol.

RESULTS 100

In silico assembly of a mitovirus sequence from NGS analysis of total RNA from a C. 101
quinoa leaf sample. 102

In order to identify a mechanically transmitted viral agent from a Hibiscus rosa-sinensis plant, 103
we submitted for NGS analysis the total RNA (depleted from ribosomal RNA) of C. quinoa leaves 104
showing chlorotic spots that were inoculated with sap from symptomatic H. rosa-sinensis plants 105
(Accession SRR8169409). Our bioinformatics pipeline (18) identified two complete virus genomes: 106
BLAST searches of viral databases identified a contig with high similarity to a tobamovirus -Hibiscus 107
latent ford pierce virus- (19), and a second contig of 2730 nt, which codes for a single putative 108
protein, from nt 322 to nt 2644 (Fig. 1). A BLAST search identified the latter as a putative mitovirus 109
RNA-dependent RNA polymerase (RdRp). Since such a contig was present also in un-inoculated C. 110
quinoa, and not in the original hibiscus plant (data not shown), we decided to provisionally name the 111
putative virus Chenopodium quinoa mitovirus 1 (CqMV1). Furthermore, to confirm absence of 112
fungal contamination (from endophytes or pathogenic fungi), assembled contigs were analyzed in 113
MEGAN 6 after DIAMOND processing for taxonomical placements of all the assembled contigs from 114
the RNAseq experiment: no fungal contigs were detected (not shown). 115

At the time when we identified the putative mitovirus (Jan 2017, deposited in the databases 116
June 22nd 2017), a tblastn search was performed by using the deduced C. quinoa mitovirus RdRp as 117
query, and when the total nr database was used, the first hits were those of a Solanum tuberosum 118
mitochondrion gene (XP_006364252; e-value 0.0, 98% query coverage, 53% amino acid identity). A 119
number of other Non-retroviral Endogenized RNA Virus Element (NERVEs), described as mitovirus-120
like sequences, are also present in the list of hits obtained by this search. Repeating the tblastn search 121
at the time of submission (October 2018), when limiting to annotated virus sequences, the highest 122
score is to a recently identified Beta vulgaris mitovirus 1 (AVH76945.1; 56% identity at the aa level, 123
82% query cover) (17) that was deposited in the database Dec 21st 2017, and a still uncharacterized 124
Ocimum basilicum RNA virus 2 sequence (YP_009408146; 32% aa identity, 49% query cover) that 125
on February 4, 2019 by guest<http://jvi.asm.org/>Downloaded from
Nerva et al. J. Virol.

was deposited in the database June 3rd 2017. To exclude that such RNA mitoviral sequences resulted 126
from transcription of a full length viral genome endogenized in C. quinoa, we investigated the 127
possible existence of a DNA fragment in the mitochondrial or nuclear DNA corresponding to the 128
assembled viral sequence. For this purpose, we designed specific primers on the predicted ORF and 129
we performed a PCR protocol on both DNA and RNA to identify in which nucleic acid fraction the 130

sequence is detectable. *C. quinoa* plants contained the viral sequence in the RNA fraction, but none of 131 them showed any specific band in the DNA fraction (Fig. 1). These results were also confirmed in a 132 more sensitive qRT-PCR protocol (not shown). 133

We then analyzed the CqMV1 amino acid sequence to identify conserved motifs. In addition 134 to the conserved RdRp domain (GDD), we detected all six conserved motifs characteristic of 135 mitoviruses (20). Due to the putative mitochondrial localization of the virus, we expected an AU 136 content > 60% because of the A-U rich nature of mitochondrial genome (21, 22) but the observed A-U 137 content is 58.39%. Whereas fungal mitoviruses typically use UGA to encode tryptophan rather than a 138 stop codon, in our case all tryptophans are encoded by UGG. 139

Stem-loop secondary structures are characteristic of 5' and 3' UTRs sequences of the positive 140 strand mitovirus genomes (3). We here analyzed presence of possible secondary structures with the 141 RNA-Fold software which revealed the presence of these structures at the 5' UTR region ($\Delta G = 33$ 142 kcal/mol; not shown). 143

We then proceeded to carry out a phylogenetic analysis that included representatives of 144 endogenized plant mitoviral sequences, characterized mitoviruses from fungi, and mitoviruses 145 characterized from other plant transcriptomes; as outgroups we included representative of the 146 Narnaviridae family and the recently proposed ourmiaviridae-like family (Fig. 2). As observed by 147 other authors, plant mitoviruses form a well-supported clade within the mitoviruses. Currently, 148 known mitoviral sequences often group according to their specific host, consistent with co-evolution 149 and infrequent interspecific transmission. 150

on February 4, 2019 by guest <http://jvi.asm.org/> Downloaded from
Nerva et al. J. Virol.

CqMV1 is differentially distributed in *C. quinoa* accession and cultivars. *Chenopodium* 151 *quinoa* is known to plant virologists because it is historically a common host-range test plant: it often 152 gives local chlorotic or necrotic lesions upon mechanical inoculation with a number of plant viruses. 153 This species is also a very important agricultural crop (23, 24) because of its resistance to a number of 154 abiotic stresses and for its nutritional value (25, 26). 155

We therefore sought to determine how widespread CqMV1 is within *C. quinoa* germplasm by 156 testing seed batches from different sources for the presence of the virus. For this purpose, initially we 157 compared *C. quinoa* accessions from different plant virology laboratories (personal collection of 158 Gancho Pasev, Maritsa Vegetable Crops Research Institute, Plovdiv, Bulgaria); later, we purchased a 159 variety of accessions from the Leibniz Institute of Plant Genetics and Crop Plant Research (IPK) and 160

from the Collection of the U.S National Plant Germplasm System (NPGS). A sensitive and fast qRT-PCR protocol was established to screen newly germinated batches of 10 plantlets for each sample. We found that the *C. quinoa* from our laboratory used as test plants in host range experiment (named in this work IPSP1), some other accessions from the Pasev collection (Supplementary on line table 1), and some common commercial cultivars (cv Regalona and cv Cherry vanilla) were positive for CqMV1. In contrast, CqMV1 did not infect 42 tested accessions from Peru and Bolivia (from the collection) (Supplementary on line table 1). Accession PI614886 (NPGS collection) from Chile is the *C. quinoa* accession used for deriving the recently published genome sequence and it carries CqMV1 (27).

CqMV1 genomic RNA accumulates preferentially in the mitochondrial fraction. Translation of CqMV1 RdRp could hypothetically occur in both the cytoplasm and the mitochondria since the same protein is encoded using both genetic codes. For this reason, we wanted to investigate if virus RNA accumulated preferentially in mitochondria-enriched preparations, compared to whole cell extracts, or to chloroplast-enriched fractions. We adapted a protocol for spinach mitochondrial enrichment and judged purity of the preparation based on chlorophyll fluorescence (Fig. 3A) and presence of specific genetic markers (ORF-X and S3 for mitochondria, S2 for a mitochondrial

on February 4, 2019 by guest <http://jvi.asm.org/> Downloaded from
Nerva et al. J. Virol.

ribosomal protein encoded by a nuclear gene, and Cox for a nuclear encoded gene). RNA was extracted from the different fractions and qRT-PCR was carried out to detect the virus and the mRNA corresponding to each of the marker genes. The virus co-purifies with mitochondrial RNAs. It is >50 fold more abundant in the mitochondrial fraction than in either the chloroplastic or the soluble cytoplasmic RNA fractions (Fig. 3B).

Evidence of minus strand CqMV1 RNA accumulation in leaf extracts. The recent contention of “contemporary” mitoviruses infecting plants (17) relies on detection of RNA transcripts corresponding to the mitovirus genome (positive RT-PCR, after DNase treatment) in the absence of a corresponding DNA segment (negative PCR). This is robust indirect evidence. Nevertheless, more direct evidence of replicating mitoviruses could come from detection of a negative strand full length RNA corresponding to the viral genome by a PCR-independent method. Therefore, a northern hybridization experiment relying on positive and minus strand run-off transcript probes to detect – strand genomic RNA and + strand genomic RNA respectively, has been performed. We used the accession BO25 as a negative control and Regalona as CqMV1 infected positive control. Our initial experiment with a first pair of + and – strand probes revealed a very abundant accumulation of a

specific positive strand CqMV1 genomic RNA band only in the virus-infected line. Attempts to detect a specific full length -strand RNA band from leaf extracts failed; only shorter virus specific RNA species could be detected by the positive strand probe designed close to the 3'end of the genome (Fig 194 4A); the presence of a specific full length -strand viral genomic RNA is likely masked by the 195 unspecific hybridization of the probe with a ribosomal band. We repeated the experiment with a 196 second pair of probes designed in a different region of the genome (Fig. 1), and in this case, we were 197 able to show a faint specific band hybridizing with the -sense genomic RNA after 15 days membrane 198 exposure to film (Fig. 4B), evidence of a minimal CqMV1 replicative activity. 199

Mechanical inoculation, seed transmission and grafting experiments. We then proceeded 200 to investigate some basic biological properties of CqMV1. Most persistent viruses are not 201 mechanically transmissible but are vertically transmissible with 100% rate through seeds. We first 202

on February 4, 2019 by guest <http://jvi.asm.org/> Downloaded from
Nerva et al. J. Virol.

sought to mechanically transmit CqMV1 from infected *C. quinoa* to accession BO25, which had 203 tested negative for CqMV1. Out of 20 inoculated plants, none showed evidence of infection in either 204 the inoculated leaf, or systemically, following standard protocols that gave 100% infection with a 205 mechanically transmissible control virus (alfalfa mosaic virus=AMV; not shown). 206

Next, we investigated the vertical transmission rate of the virus in plantlets germinated from 207 seeds obtained from infected plants (IPSP1 and cv Regalona). We tested individually 100 plantlets for 208 each accession by qRT-PCR and all tested positive. Finally, we tested the possibility of transmitting 209 CqMV1 through grafting, which often overcomes the mechanical transmission limitations of non-210 mechanically transmissible viruses. We grafted healthy BO25 on IPSP1 rootstocks (6 plants). We then 211 tested the scion and graft at 1 and 2 months after grafting. CqMV1 could not be detected in any 212 grafted scion systemically, but its presence was confirmed in all the infected rootstocks. 213

Differential symptom severity of pathogenic virus infections on CqMV1-infected and 214 CqMV1-free *C. quinoa* lines. We focused our experiments on the accessions BO25 and BO78 as 215 negative controls and IPSP1 and Regalona as CqMV1 infected positive controls since they did not 216 show any evident phenotypic differences in our environmental growth conditions. We wanted to test if 217 the presence/absence of the mitovirus has any synergistic or antagonistic effect once the plants are 218 inoculated with a disease-causing plant virus. In particular, the four accessions have been infected 219 with three different pathogenic viruses able to replicate, systemically infect and induce symptoms on 220 *C. quinoa* plants: i) an isolate of AMV, ii) an isolate of lettuce mosaic virus (LMV) and iii) an isolate 221

of hibiscus latent ringspot virus (HLRSV). 222

Leaves of virus-inoculated plants were compared to leaves of mock-inoculated plants 7 days 223

post infection (dpi): for both AMV and HLRV we observed local chlorotic lesions indistinguishable 224

between the CqMV1-infected lines and the CqMV1-free lines (Fig. 5A and Fig. 5C). In contrast, 225

leaves of plants infected with LMV displayed local chlorotic lesions when the leaves came from 226

CqMV1-infected lines, but more severe local necrotic lesions in leaves from CqMV-free lines (Fig. 227

5B). 228

on February 4, 2019 by guest<http://jvi.asm.org/>Downloaded from

Nerva et al. J. Virol.

We then repeated symptoms observation on whole plants at 14 dpi. The CqMV1-infected lines 229

IPSP1 and Regalona displayed milder systemic symptoms (Fig. 6D-E-F and Fig. 6J-K-L) compared to 230

the CqMV1-free lines BO25 and BO78 (Fig. 6G-H-I and Fig. 6A-B-C). All four lines showed 231

comparable mild growth impairment, leaf malformation and mild mottling in upper uninoculated 232

leaves. Nevertheless, the most evident specific differential phenotype associated to CqMV1 233

presence/absence is the red-violet stem pigmentation observed in CqMV1-free lines (Fig. 6M). 234

Conversely, mock inoculated or CqMV1-infected plants did not show stem pigmentation (Fig. 6N). 235

Differential small RNA accumulation and processing of AMV and CqMV1 in infected C. 236

quinoa plants. A number of fungal mitoviruses have been discovered through sRNA characterization, 237

suggesting that--at least in fungi--they are subject to RNAi processing (28, 29). In order to 238

characterize the sRNA present in C. quinoa we decided to compare three libraries of sRNA: i) from 239

CqMV1-free BO25 infected by AMV (Accession SRR8169660); ii) mock-inoculated cv. Regalona 240

carrying CqMV1 (Accession SRR8169658); iii) cv Regalona mechanically infected with AMV 241

(Accession SRR8169659). Using a bioinformatic pipeline that was previously used to assemble de 242

novo virus genomes (18, 30), we first confirmed that accession BO25 does not carry any virus other 243

than AMV, whereas the same pipeline could assemble CqMV1 from cv Regalona and AMV from 244

AMV-infected cultivars. When we looked at the percentage of total sRNA that mapped to the two 245

viral full length sequences we noticed that, for plant mitovirus, the percentage is very low compared to 246

AMV (Table 1), even if the overall genomic RNA is actually more abundant based on qRT-PCR 247

assessment and northern blot (not shown). We then proceeded to look at the size distribution of the 248

sRNA. The availability of the C. quinoa genome (27, 31) allowed us to assess reads mapping to the 249

host genome (with a characteristic peak at 24 nt length common to most plants) and to each of the two 250

viruses. In the case of AMV a typical peak corresponding to 21 nt length (47% of the reads) and a 251

minor 22 nt length peak (30% of the reads) are likely the hallmark of a Dicer and RISC mediated anti-252

viral response (Fig. 7). Surprisingly, in the case of reads mapping to CqMV, a sharp peak for the 16 nt 253
long reads corresponding to 30% of the reads was present, whereas the peaks corresponding to 21 and 254
on February 4, 2019 by guest<http://jvi.asm.org/>Downloaded from
Nerva et al. J. Virol.

22 nt long reads were both below 10% (Fig. 7). Availability of *C. quinoa* chloroplast (32), and nuclear 255
(27) genomes and our own selection of a number of mitochondrial genes from our transcriptome data, 256
allowed us to check the read-distribution lengths of host sRNA mapping to those genomes. Small 257
RNA mapping onto the chloroplast genome had a major peak at 27 nt length (22%), whereas the 258
second peak is at the 22 nt; in the case of sRNA mapping to mitochondrial genes (in this case only the 259
putative coding sequences were used), a sharp peak is present for 16 nt length (67% of the sRNA). 260
The N terminal nucleotide distribution of reads mapping to CqMV and AMV were A=30.5% 261
C=12.9% G=37.7% U=18.9% and A=25.6% C=16.3% G=10.2% U=47.9%, respectively. 262
We then performed an sRNA miner analysis on reads mapping on the CqMV1 genome to 263
reveal clustered organellar sRNA (cosRNA), which are putative footprints of RNA binding proteins 264
(RBP): using conservative settings we were able to detect eight different footprints from 4 distinct 265
peaks (Supplementary on line Fig. 1). Therefore, sRNA analysis seems to confirm that most of the 266
CqMV1 RNA is likely protected from dicer/RISC mediated viral anti-silencing response inside the 267
mitochondria, where distinct processing occurs resulting mostly in 16 nt length sRNA. 268
269

DISCUSSION 270

Plant mitoviruses, a new class of cryptic (persistent) plant viruses 271
Our work confirms the recent finding that plant mitochondrial viruses exist not only as 272
widespread endogenized sequences in mitochondrial or nuclear genomes (13), but also as true virus 273
encoded RdRp-depending replicating RNA elements (17). Here we provide further molecular 274
evidence through detection of minus strand RNA. We can also exclude that such a replicating virus is 275
carried by a fungal endophyte based on RNAseq analysis, as our dataset lacks of any fungal reads. 276
Our work is the first to provide evidence that bona fide plant mitoviruses are enriched in plant 277
mitochondria. 278
This is not the first case of a virus associated with plant mitochondria. The plant virus 279
carnation Italian ringspot virus replicates on mitochondrial external membranes and causes 280
on February 4, 2019 by guest<http://jvi.asm.org/>Downloaded from
Nerva et al. J. Virol.

multivesicular body alterations of mitochondria (33) but particles and RNA readily accumulate in the 281
cytoplasm, and replicases (p35 and co-terminal p95) targeted to the external membrane of 282
mitochondria have N and C termini on the cytosolic side (33), so this virus is best viewed as 283
cytoplasmic. 284

We also note that viruses have already been characterized from chloroplasts and mitochondria 285
of the green alga *Bryopsis* sp. (34), specifically, a mitochondrial virus related to fungal totiviruses (35) 286
and a chloroplastic virus related to the partitiviruses (36); both viruses have a typical dsRNA genome 287
and have no phylogenetic relationship with any known bacterial. In contrast, plant mitoviruses, 288
including CqMV1, are instead phylogenetically related to the phage family Leviviridae. 289

Our phylogenetic analysis would suggest a comprehensive review of the taxonomy of 290
mitoviruses. Inclusion of a number of well-characterized fungal and plant narna-like viruses and 291
members of the family Leviviridae in the phylogenetic analysis makes it evident that mitoviruses are 292
monophyletic. Their wide diversity warrants the establishment of a family taxon called Mitoviridae, 293
separated from the family Narnaviridae. The newly established family would comprise a number of 294
subfamilies and genera, including the very distantly related mitovirus species characterized from the 295
arbuscular mycorrhizal fungus *Gigaspora margarita* which are included in a clade basal to existing 296
characterized mitoviruses (37). As already observed by other authors (17), plant mitovirus are nested 297
in a specific fungal mitovirus clade, therefore raising questions about the evolutionary trajectory of 298
plant mitoviruses which has been discussed at length elsewhere (17). 299

We provide here for the first time a basic biological characterization of a plant mitovirus, 300
which has the typical features of cryptic viruses: they cannot be transmitted horizontally by 301
mechanical inoculation or grafting, whereas they are transmitted vertically at a 100% rate through 302
seeds. Lack of transmission through grafting is indeed an expected result for mitoviruses that replicate 303
in plant mitochondria, since movement of mitochondria through the plant is likely minimal and will 304
not replace existing population of mitochondria. This is somewhat different to what observed in fungi 305

on February 4, 2019 by guest <http://jvi.asm.org/> Downloaded from
Nerva et al. J. Virol.

where “grafting” (hyphal fusion through anastomoses) was shown to allow mitovirus transmission in 306
some cases (38). 307

The high level of seed transmission observed in this study is also expected, as seeds formed on 308
infected plants must inherit their parents’ infected mitochondria. Plants have mechanisms to ensure 309
that mitochondria are only maternally inherited and to maintain low heteroplasmy levels. 310

Nevertheless, there is evidence of biparental transmission of mitochondria in plants (39). *C. quinoa* is normally self-pollinating in nature, but studies of mitochondrial inheritance could potentially be carried out through artificial mechanical emasculation and forced crosses (40). An important avenue of future work will therefore be creation of reciprocal crosses with mitovirus-infected and mitovirus-free maternal and paternal lines to allow isolation of quasi-isogenic plants differing only for the mitochondrial/viral content.

Absence of a movement protein in mitovirus genomes and lack of a movement-complementing virus in CqMV1 infected *C. quinoa* also supports the idea that they can infect all type of cells, including meristematic ones, as is the case of other cryptic viruses (41).

The existence of cryptic viruses in plants was known for at least four decades, since their discovery in a number of different plant species at the end of the 1970s (41). Currently known persistent/cryptic plant viruses include members of five families: Partitiviridae (42-44), Totiviridae (45, 46), Chrisoviridae (47, 48) Endornaviridae (49) and Amalgaviridae (50-53). We here provide convincing evidence that plant mitoviruses should be also defined as cryptic (persistent) viruses. The fact that CqMV1 is present in commercial varieties of *C. quinoa* (Regalona and Cherry Vanilla), but that a number of other accessions from Bolivia and Peru do not carry any mitovirus, seems to support the idea that they cause no specific harm to their host. Moreover, the widespread occurrence of mitoviruses in domesticated material raises the possibility of their beneficial role in specific agro-ecological niches. Recent reviews and metagenomics studies unveiled the widespread occurrence of cryptic (persistent) viruses in plants and other authors have discussed a possible beneficial role for their host (54-56). In particular some studies have looked at the presence of endornavirus as it relates

on February 4, 2019 by guest <http://jvi.asm.org/> Downloaded from
Nerva et al. J. Virol.

to the domestication of pepper (49). There is also growing evidence that other plant viruses, which are not defined as cryptic since in some specific instances they can cause obvious symptoms, can indeed provide advantages to their host in resistance to abiotic stress: an example is grapevine rupestris stem pitting associated virus (GRSPaV) where a molecular mechanism has also been proposed (58, 59).

A preliminary experiment to detect differential symptom reaction to a panel of viruses systemically infecting *C. quinoa* did not reveal any major synergistic or antagonistic effect caused by CqMV1 mitochondrial infection. Nevertheless, some interesting features in specific virus-plant interactions should be pointed out: the enhanced necrotic hypersensitive reaction and the stem pigmentation in the absence of CqMV1 implies that infection with the mitovirus can somehow ameliorate the symptoms of at least some other viruses. We can speculate that the presence of CqMV1 in the mitochondria

might alter the oxidative stress cellular signaling resulting in necrosis and pigment accumulation. 342
 Further classes of biotic and abiotic stress should be tested, in view of the fact that mitochondria are 343
 central in a number of stress related phenomena in plants, particularly in the roots mediating tolerance 344
 to harsh environments (60). 345
 Numerous attempts to isolate CqMV1 dsRNA from infected plants have failed, using a protocol 346
 previously described (61) and using as positive control tomato mosaic virus infected *C. quinoa* and the 347
 fungal isolate MUT4330 previously described (61). Lack of detectable dsRNA in CqMV1-infected *C. 348*
quinoa could be due to the extreme toxicity of dsRNA to plant mitochondria, as recently observed for 349
 dsRNA expressed in mitochondria in human cell lines: a specific degradation pathway prevents the 350
 export of dsRNA and the onset of a general anti-viral defense driven by MDA5 dependent anti-viral 351
 signaling (62). 352
 Differential RNA processing inside mitochondria and evidence of a yet undefined anti-viral 353
 response 354
 Our sRNA analysis indicates that the mitochondrial virus present in *C. quinoa* is not subject to 355
 the Dicer/argonaute dependent anti-viral silencing response that typically targets plant viruses (63). 356
 This is not due to a defective silencing response in *C. quinoa*, because we provided evidence that the 357
 on February 4, 2019 by guest <http://jvi.asm.org/> Downloaded from
 Nerva et al. J. Virol.

typical Dicer/argonaute processing occurs in the same AMV-infected *C. quinoa* plant extract. This 358
 raises the question of what might limit mitochondrial virus replication in plants and fungi, where 359
 mitoviruses occur. Silencing of fungal mitoviruses is not well characterized, but two recent studies 360
 show that mitoviral sRNA generated in fungi is not different from that generated from cytoplasmic 361
 viruses in either quality or quantity (28, 29). Our discovery that plants accumulate very low amounts 362
 of mitovirus sRNA and that these are most frequently 16 nt in length is a major difference with fungal 363
 systems and raises the question of what molecular pathway generates such a specific sRNA size 364
 distribution. Furthermore, the significant differences in the N terminal nucleotide of reads mapping to 365
 CqMV and to AMV also point to distinct degradation machineries for the two viruses. Our data 366
 suggest that the 16nt mitoviral sRNA likely result from a non-viral specific RNA degradation process, 367
 since size distribution of sRNA generated from mRNAs expressed from the mitochondrial genome 368
 shows the same peak at 16nt. In this respect, the combined roles of exoribonucleases such as PNPase 369
 and RNR1 and RNA binding proteins in leaving footprints of various lengths could be at the basis of 370
 this differential sRNA accumulation, consistent with recent studies of size distribution footprints in 371

chloroplast and mitochondrial RNA transcripts in *Arabidopsis thaliana* (64). Previous authors 372
hypothesized a possible regulatory role of the sRNA resulting from processing by Pentatricopeptide 373
Repeat proteins (PPR proteins, a subset of RBP proteins typical of plants) (64, 65), providing 374
therefore a testable model of anti-viral defense based on intra-mitochondrial sRNA generation. 375
From an evolutionary perspective, it would be interesting to look at bacterial anti-viral 376
responses against RNA viruses (RNA phages). Recent work has shown that RNA bacteriophage 377
diversity is much higher than previously thought (66): while current taxonomy has only two family of 378
prokaryotic RNA viruses, the Leviviridae and the Cystoviridae, indirect evidence indicates that some 379
Picobirnaviridae are bacterial viruses (67). In this respect also new anti-viral defense systems are 380
constantly unveiled (68). Although RNA-guided RNA cleavage by a specific CRISPR RNA-Cas 381
system is known (69), its role in specific anti-viral response in natural systems has yet to be shown 382
on February 4, 2019 by guest <http://jvi.asm.org/> Downloaded from
Nerva et al. J. Virol.

(70, 71); nevertheless, in an in vitro heterologous system a type III-A CRISPR-Cas system will restrict 383
MS2 RNA phage infection (72). 384
Future work will pursue further biochemical characterization of the sRNA response to 385
mitovirus infection in different biological systems (fungi and plants) and the analysis of possible 386
differential physiological reactions linked to mitovirus infection in plants experiencing harsh 387
environmental stress conditions. 388
389

MATERIALS AND METHODS 390

Plant material and RNA sequencing. Plant seeds used in this study (accession, seeds from 391
personal collections and from public repositories) are described in detail in Supplementary online 392
Table 1. 393
Total RNA extraction from IPSP1 plants was performed using the Spectrum Plant Total RNA Kit 394
(Sigma-Aldrich, Saint Louis, MO, USA) following manufacturer instructions. RNA quantification and 395
quality were tested using NanoDrop 2000 Spectrophotometer (Thermoscientific, Waltham, MA, 396
USA). Macrogen Europe (Amsterdam, Netherlands) performed ribosomal RNA (rRNA) depletion 397
using the Ribo-Zero™ Plant Kit (Epicentre, Madison, WI, USA), library construction and sequencing 398
using an Illumina HiSeq4000. 399
For mechanical inoculation experiments we used three different virus species, belonging to 400
different families, that systemically infect *C. quinoa*: the LMV, family Potyviridae, genus Potyvirus 401
(Dim 60, PLAVIT collection), AMV, family Bromoviridae, genus Alfamovirus (IFA 30, PLAVIT 402

collection) and HLRSV, family Secoviridae, genus Nepovirus (VE 453, PLAVIT collection). 403
 Bioinformatics analysis and molecular validation. Raw reads obtained from total RNA 404
 sequencing were assembled into contigs using Trinity 2.3.2 (73) and virus were identified as 405
 already described (18) using Blast+ suite 2.6.0 (74), BWA 0.7.15-r1140 (75) and samtools 1.3 (76). 406
 Once viral sequences were identified specific primers were designed (Supplementary on line 407
 Tab. 3) to reveal the molecular nature (if DNA, RNA or both). To detect viral sequence possibly 408
 on February 4, 2019 by guest <http://jvi.asm.org/> Downloaded from
 Nerva et al. J. Virol.

integrated into in the host genome (both nuclear or mitochondrial) we performed a total nucleic acid 409
 extraction using a phenol-chloroform protocol (77). We then performed, on half of the volume, a 410
 digestion with RNase A (four hours) to completely remove any trace of RNAs. The second half of the 411
 total nucleic acid extraction was subjected to a four-hour DNase treatment in order to completely 412
 remove all traces of DNA. The DNased RNA was then used in a retrotranscription (RT) reaction in 413
 order to obtain cDNA suitable for PCR. We then performed PCR with specific primers for both an 414
 internal control (COX) and for the viral sequence using as template the obtained DNA and cDNA 415
 samples from the four C. quinoa lines (IPSP1, Regalona, BO25 and BO78). The same templates were 416
 used in quantitative retrotranscriptase PCR (qRT-PCR) with specific primers to evaluate presence and 417
 quantities of the internal control and the viral sequence in the four different lines. 418
 PCR products for viral sequence were cleaned with DNA clean & concentrator™-5 kit 419
 (Zymoresearch, CA, USA), cloned into pGEM-T easy vector (Promega, Madison, WI, USA) and 420
 sequenced at Bio-Fab Research (Rome, Italy). 421
 The 5' and 3' terminal sequences were obtained through the RACE protocol. Presence of possible 422
 secondary structure was evaluated using RNAfold (78). 423
 To identify possible contamination with fungal sequences in our RNAseq experiments we 424
 analyzed taxonomic placement of all the assembled contigs using MEGAN6 software (79). 425
 Small-RNA sequencing and analysis. To detect CqMV1 small RNAs (sRNAs) we started 426
 from total RNA extraction of mock inoculated accession Regalona and Regalona infected by AMV. In 427
 parallel BO78 accession infected by AMV was used as negative CqMV1 control. Total RNA from the 428
 three samples were sent to the Italian Institute for Genomic Medicine (IIGM, Turin, Italy) where 429
 sRNAs were isolated, library constructed and then sequenced using a MiSeq System (Illumina Inc., 430
 San Diego, CA, USA). 431
 Raw reads were cleaned from adaptor, quality filtered using the FASTX-toolkit 432

(http://hannonlab.cshl.edu/fastx_toolkit/index.html) and then assembled using Velvet (80) and Oases (81). Contigs were used in blastx and blastn searches against a custom database to identify viral sequences. To determine the sRNA size distribution on viral genomes (both CqMV1 and AMV) we used BWA and samtools to map raw reads against the two viral genomes and we then filtered for reads length through a custom Perl script. Due to the unexpected pattern of sRNA mapping on CqMV1 genome we decided to map also raw reads against C. quinoa genes. For nuclear and chloroplast genes representation we used the genome assembly GCF_001683475.1 and NC_034949.1. Due to absence of available mitochondrial genome assembly for C. quinoa we created a custom database containing gene sequences of mitochondrial origin retrieved from the total RNA sequencing by comparing with Arabidopsis thaliana mitochondrial genome (NC_037304.1). The relative frequency of each nucleotide at 5' N-terminal position of the small RNAs was calculated using Galaxy tools.

on February 4, 2019 by guest <http://jvi.asm.org/> Downloaded from
Nerva et al. J. Virol.

We performed an analysis for clustered organellar sRNA using sRNA miner, implemented in R/Bioconductor using as parameter 40 for the minimal reads for end and 0.85 for the sharpness of end.

Phylogenetic analysis. Predicted ORF encoding for RdRp were used to build an alignment using MUSCLE algorithm implemented in MEGA 6. Phylogenetic tree was built using the maximum likelihood method, aligned protein sequences were used to estimate the best substitution rate and parameter with MEGA 6. Substitution pattern and rates were estimated under the model designed by Dimmic (+Gamma +Invar +Freq). One thousand bootstrap replicates were performed and branches with bootstrap value under 50 have been collapsed. A list of the accession numbers of the viruses contained in the tree is shown in supplementary table 2.

We performed an analysis for clustered organellar sRNA using sRNA miner, implemented in R/Bioconductor (83) using as parameter 40 for the minimal reads for end and 0.85 for the sharpness of end.

Phylogenetic analysis. Predicted ORF encoding for RdRp were used to build an alignment using MUSCLE algorithm implemented in MEGA 6 (84). Phylogenetic tree was built using the maximum likelihood method, aligned protein sequences were used to estimate the best substitution rate and parameter with MEGA 6. Substitution pattern and rates were estimated under the model designed by Dimmic (+Gamma +Invar +Freq) (85). One thousand bootstrap replicates were performed and branches with bootstrap value under 50 have been collapsed. A list of the accession numbers of the viruses contained in the tree is shown in supplementary table 2.

Mitochondrial and Chloroplast enrichment protocol and quantitative evaluation of

CqMV1 and marker genes. Chloroplast and mitochondria enriched fractions were obtained by a modified protocol already used for cucumber plants (86, 87). Ten grams of C. quinoa leaves were homogenized in the ratio 1:10 in chilled extraction buffer (Sucrose 0.45 M, MOPS 15mM, EGTA 1.5mM, pH 7.4 with KOH) added with PVP 0.6%, BSA 0.2%, DTT 10mM and PMSF 0.2mM. After filtration on Miracloth (Calbiochem) the homogenate was centrifuged at 2000g for 5 min to separate

on February 4, 2019 by guest <http://jvi.asm.org/> Downloaded from
Nerva et al. J. Virol.

chloroplasts and cell debris. Pellet was used for the subsequent chloroplast purification; instead, the 461 supernatant was again centrifuged at 13000g for 30 min to obtain the mitochondrial fraction in the 462 pellet. From this point, the protocol followed two different ways. 463

Crude chloroplasts pellet were suspended in 1 ml of sorbitol resuspension buffer (SRM, 464 Sorbitol 1.65M, Hepes 250 mM pH8 with KOH) and layered on a Percoll® (Sigma-Aldrich) gradient 465 (35% buffer and 80% in SRM) and centrifuged at 2600g in a swing out rotor (SW41 Beckman) for 10 466 min. After centrifugation, the fraction with chloroplast was collected with a Pasteur pipette, diluted in 467 30 ml of SRM buffer and centrifuged at 2000g for 5 min, to remove all the Percoll. This step was 468 repeated for two times. Pellet was then suspended in resuspension buffer (RB, Mannitol 0.4 M, Mops 469 10 mM, EGTA 1 mM, pH 7.2) added with PMSF 0.2 mM, and checked on the microscope to evaluate 470 the purity of the preparation. Crude mitochondria pellet was resuspended in 1 ml of washing buffer 471 (WB; sucrose 0.6 M, Mops 20 mM, EGTA 2 mM, pH 7.2 with KOH) added with PMSF 0.2 mM, 472 layered on a Percoll gradient (18%, 23% and 40% in WB) and centrifuged at 12000g in SW21 473 (Beckmann) for 45 min. Mitochondrial fraction, between the 23% and 40% interface, was collected 474 with a Pasteur pipette and two wash-step were performed as already described for chloroplasts in WB. 475 We resuspended pellet in about 0.1 ml and checked the quality of purification by observation with 476 fluorescent microscope. Mitochondrial and chloroplast enriched fractions were stored at -80°C until 477 use for RNA extraction and qRT-PCR analysis. In order to check which fraction contained virus 478 genome enrichments, RNA was extracted using the Spectrum™ plant total RNA kit (Sigma-Aldrich, 479 Saint Louis, MO, USA) from preparations representing normalized amounts of each fraction. 480

Complementary DNA (cDNA) was synthesized using the High Capacity cDNA Reverse Transcription 481 Kit (Applied Biosystems, Foster city, CA, USA). We then tested the presence of virus genomic RNA 482 and mRNA corresponding to a number of marker genes with quantitative real time PCR using a 483 CFX96™ apparatus (Biorad, Hercules, CA, USA) and iTaq™ Universal Probes and iTaq™ Universal 484 SYBR Supermixes (Biorad) following protocols previously described (88). The marker genes 485 corresponded to sequences of the Cytochrome P450 oxydase (ANY30855.1); the S2 ribosomal 486

on February 4, 2019 by guest <http://jvi.asm.org/> Downloaded from
Nerva et al. J. Virol.

protein, present in the mitochondria but encoded by the nuclear genome (89); the S3 ribosomal 487 protein, encoded by plant mitochondrial genomes (90); the ORF-X protein, also encoded by 488 mitochondrial genomes (91); C. quinoa sequences related to the latter three genes were retrieved from 489 our RNAseq database. Oligonucleotides used for qRT-PCR are displayed in Supplementary on line 490 table 3. 491

Northern blot analysis. For Northern blot analyses, total RNA from leaves of different age 492
 was prepared using Total Spectrum RNA Reagent (Sigma-Aldrich) as suggested by the manufacturer. 493
 RNA samples were separated in denaturing conditions (glyoxal method) as detailed, using HEPES-494
 EDTA buffer (92). Radio-labeled probes were prepared from linearized plasmid containing the cDNA 495
 clones (producing probes in both orientation) through T7 transcription using the Maxiscript T7 kit 496
 reagents (Thermo Fisher Scientific Inc., Waltham, MA, USA) as suggested by manufacturer. 497
 qRT-PCR fast screening method. For a fast screening of viral infection we applied 498
 modifications of a simple qRT-PCR protocol that uses crude extracts as template (93). We placed 30 499
 seeds to germinate in 90 mm diameter Petri dishes with wet filter paper and let it germinate for 3 days 500
 (or single plantlets in the case of seed transmission assay). Plantlets of all the accession tested were 501
 placed in extraction bags (Bioreba, Reinach, Switzerland) and diluted 1:20 (w/v) with carbonate buffer 502
 pH 9.6 (94) added with 2% PVP40, 0.2% BSA, 1% sodium metabisulfite and 0.05% tween 20. Raw 503
 extract has been diluted 1:10 in sterile water and boiled 10 min at 95 °C. qRT-PCR screening was 504
 performed using a CFX96™ Real-Time PCR Detection System (Biorad), PCR mix was prepared with 505
 iTaq™ Universal Probes Supermix (Biorad) adding 3 U of reverse transcriptase from High-Capacity 506
 RNA-to-cDNA Kit (Thermo Fisher Scientific) for each sample. Reactions have been performed in 10 507
 µl of total volume adding 1 µl of boiled extract to 9 µl of PCR mix. The qRT-PCR protocol has a 30 508
 min step at 37°C to perform the reverse transcription of the viral genome, then is followed by 1 min at 509
 94 °C and 40 steps of denaturation at 95 °C for 10 sec, annealing and extension at 60 °C for 30 sec. 510
 Data availability. The GenBank/EMBL/DDBJ accession numbers of the sequences reported 511
 in this paper is MF375475. 512

on February 4, 2019 by guest<http://jvi.asm.org/>Downloaded from
 Nerva et al. J. Virol.

513
 514

ACKNOWLEDGMENTS 515

We thank Caterina Perrone and Elena Zocca for excellent technical assistance in the greenhouse work, 516
 Riccardo Lenzi for mitochondrial enrichment preparation, Marco Chiapello for helping with the 517
 implementation of the sRNA miner analysis and Dr. Doug Grubb for editing the manuscript. 518
 This work was supported in part by the European Union's Horizon H2020 Research and 519
 Innovation Programme, Grant Agreement N. 773567. 520

on February 4, 2019 by guest<http://jvi.asm.org/>Downloaded from
 Nerva et al. J. Virol.

REFERENCES

1. Hillman BI, Cai G. 2013. The family Narnaviridae: simplest of RNA viruses. *Adv Virus Res* 86:149-176. 522
2. Polashock JJ, Hillman BI. 1994. A small mitochondrial double-stranded (ds) RNA element associated with a 523 hypovirulent strain of the chestnut blight fungus and ancestrally related to yeast cytoplasmic T and W dsRNAs. *Proc Natl Acad Sci U S A* 91:8680-8684. 525
3. Xu Z, Wu S, Liu L, Cheng J, Fu Y, Jiang D, Xie J. 2015. A mitovirus related to plant mitochondrial gene confers 526 hypovirulence on the phytopathogenic fungus *Sclerotinia sclerotiorum*. *Virus Res* 197:127-136. 527
4. Nibert ML. 2017. Mitovirus UGA(Trp) codon usage parallels that of host mitochondria. *Virology* 507:96-100. 528
5. Turina M, Hillman BI, Izadpanah K, Rastgou M, Rosa C, Consortium IR. 2017. ICTV Virus Taxonomy Profile: 529 Ourmiavirus. *J Gen Virol* 98:129-130. 530
6. Dolja VV, Koonin EV. 2018. Metagenomics reshapes the concepts of RNA virus evolution by revealing 531 extensive horizontal virus transfer. *Virus Res* 244:36-52. 532
7. Raven PH. 1970. A multiple origin for plastids and mitochondria. *Science* 169:641-646. 533
8. Koonin EV, Dolja VV, Krupovic M. 2015. Origins and evolution of viruses of eukaryotes: the ultimate 534 modularity. *Virology* 479-480:2-25. 535
9. Koonin EV, Dolja VV. 2014. Virus world as an evolutionary network of viruses and capsidless selfish elements. 536 *Microbiol Mol Biol Rev* 78:278-303. 537
10. Kondo H, Chiba S, Suzuki N. 2015. Detection and Analysis of Non-retroviral RNA Virus-Like Elements in Plant, 538 Fungal, and Insect Genomes. In: Uyeda I., Masuta C. (eds) *Plant Virology Protocols. Methods in Molecular Biology* 539 (Methods and Protocols), vol 1236. Humana Press, New York, NY 540
11. Horie M, Honda T, Suzuki Y, Kobayashi Y, Daito T, Oshida T, Ikuta K, Jern P, Gojobori T, Coffin JM. 2010. 541 Endogenous non-retroviral RNA virus elements in mammalian genomes. *Nature* 463:84-87. 542
12. Katzourakis A, Gifford RJ. 2010. Endogenous viral elements in animal genomes. *PLoS Genet* 6:e1001191. 543
13. Bruenn JA, Warner BE, Yerramsetty P. 2015. Widespread mitovirus sequences in plant genomes. *PeerJ* 3:e876. 544
14. Leister D, Kleine T. 2011. Role of intercompartmental DNA transfer in producing genetic diversity. *Int Rev Cell* 545 *Mol Biol* 291:73-114. 546
15. Marienfeld JR, Unseld M, Brandt P, Brennicke A. 1997. Viral nucleic acid sequence transfer between fungi and 547 plants. *Trends Genet* 13:260-261. 548
16. Goremykin VV, Salamini F, Velasco R, Viola R. 2008. Mitochondrial DNA of *Vitis vinifera* and the issue of 549 rampant horizontal gene transfer. *Mol Biol Evol* 26:99-110. 550
17. Nibert ML, Vong M, Fugate KK, Debat HJ. 2018. Evidence for contemporary plant mitoviruses. *Virology* 551 518:14-24. 552
18. Nerva L, Varese GC, Turina M. 2018. Different Approaches to Discover Mycovirus Associated to Marine 553 Organisms. In: Pantaleo V., Chiumenti M. (eds) *Viral Metagenomics. Methods in Molecular Biology*, vol 1746. Humana 554 Press, New York, NY 555
19. Nerva L, Vallino M, Turina M, Ciuffo M. 2018. Identification and characterization of Hibiscus latent Fort Pierce 556 virus in Italy. *J Plant Pathol* 100:145-145. 557
20. Hong Y, Dover SL, Cole TE, Brasier CM, Buck KW. 1999. Multiple Mitochondrial Viruses in an Isolate of the 558 Dutch Elm Disease Fungus *Ophiostoma novo-ulmi*. *Virology* 258:118-127. 559
21. Hong Y, Cole TE, Brasier CM, Buck KW. 1998. Evolutionary Relationships among Putative RNA-Dependent 560 RNA Polymerases Encoded by a Mitochondrial Virus-like RNA in the Dutch Elm Disease Fungus, *Ophiostoma novo-ulmi*, by Other Viruses and Virus-like RNAs and by the Arabidopsis Mitochondrial Genome. *Virology* 246:158-169. 562
22. Paquin B, Laforest M-J, Forget L, Roewer I, Wang Z, Longcore J, Lang BF. 1997. The fungal mitochondrial 563 genome project: evolution of fungal mitochondrial genomes and their gene expression. *Curr. Genet.* 31:380-395. 564
23. Bazile D, Jacobsen S-E, Verniau A. 2016. The Global Expansion of Quinoa: Trends and Limits. *Front Plant Sci* 565 7:622. 566
24. Skarbo K. 2015. From Lost Crop to Lucrative Commodity: Conservation Implications of the Quinoa Renaissance. 567 *Hum Organ* 74:86-99. 568
25. Vega-Galvez A, Miranda M, Vergara J, Uribe E, Puente L, Martinez EA. 2010. Nutrition facts and functional 569 potential of quinoa (*Chenopodium quinoa* willd.), an ancient Andean grain: a review. *J Sci Food Agric* 90:2541-2547. 570
26. Jacobsen SE, Mujica A, Jensen CR. 2003. The resistance of quinoa (*Chenopodium quinoa* Willd.) to adverse 571 abiotic factors. *Food Reviews International* 19:99-109. 572
27. Jarvis DE, Ho YS, Lightfoot DJ, Schmockel SM, Li B, Borm TJA, Ohyanagi H, Mineta K, Michell CT, Saber N, 573 Kharbatia NM, Rupper RR, Sharp AR, Dally N, Boughton BA, Woo YH, Gao G, Schijlen EGWM, Guo X, Momin AA, 574 Negrão S, Al-Babili S, Gehring C, Roessner U, Jung C, Murphy K, Arold ST, Gojobori T, van der Linden CG, van Loo 575 EN, Jellen EN, Maughan PJ, Tester M. 2017. The genome of *Chenopodium quinoa*. *Nature* 542:307-312. 576
28. Donaire L, Ayllon MA. 2017. Deep sequencing of mycovirus-derived small RNAs from *Botrytis* species. *Mol* 577 *Plant Pathol* 18:1127-1137. 578

on February 4, 2019 by guest <http://jvi.asm.org/> Downloaded from
Nerva et al. J. Virol.

29. Munoz-Adalia EJ, Diez JJ, Fernandez MM, Hantula J, Vainio EJ. 2018. Characterization of small RNAs 579 originating from mitoviruses infecting the conifer pathogen *Fusarium circinatum*. *Arch Virol* 163:1009-1018. 580
30. Margaria P, Miozzi L, Ciuffo M, Pappu HR, Turina M. 2015. The first complete genome sequences of two 581 distinct European tomato spotted wilt virus isolates. *Arch Virol* 160:591-595. 582
31. Zou C, Chen A, Xiao L, Muller HM, Ache P, Haberer G, Zhang M, Jia W, Deng P, Huang R, Lang D, Li F, Zhan 583 D, Wu X, Zhang H, Bohm J, Liu R, Shabala S, Hedrich R, Zhu J-K, Zhang H. 2017. A high-quality genome assembly of 584 quinoa provides insights into the molecular basis of salt bladder-based salinity tolerance and the exceptional nutritional 585 value. *Cell Res* 27:1327-1340. 586
32. Hong S-Y, Cheon K-S, Yoo K-O, Lee H-O, Cho K-S, Suh J-T, Kim S-J, Nam J-H, Sohn H-B, Kim Y-H. 2017. 587 Complete Chloroplast Genome Sequences and Comparative Analysis of *Chenopodium quinoa* and *C. album*. *Front Plant Sci* 8:1696. 589
33. Weber-Lotfi F, Dietrich A, Russo M, Rubino L. 2002. Mitochondrial targeting and membrane anchoring of a viral 590 replicase in plant and yeast cells. *J. Virol.* 76:10485-10496. 591
34. Ishihara J, Pak JY, Fukuhara T, Nitta T. 1992. Association of particles that contain double-stranded RNAs with 592 algal chloroplasts and mitochondria. *Planta* 187:475-482. 593
35. Koga R, Fukuhara T, Nitta T. 1998. Molecular characterization of a single mitochondria-associated double-594 stranded RNA in the green alga *Bryopsis*. *Plant Mol Biol* 36:717-724. 595
36. Koga R, Horiuchi H, Fukuhara T. 2003. Double-stranded RNA replicons associated with chloroplasts of a green 596 alga, *Bryopsis cinicola*. *Plant Mol Biol* 51:991-999. 597
37. Turina M, Ghignone S, Astolfi N, Silvestri A, Bonfante P, Lanfranco L. 2018. The virome of the arbuscular 598 mycorrhizal fungus *Gigaspora margarita* reveals the first report of DNA fragments corresponding to replicating non-599 retroviral RNA viruses in Fungi. *Environ Microbiol* 20:2012-2025. 600
38. Polashock JJ, Bedker PJ, Hillman BI. 1997. Movement of a small mitochondrial double-stranded RNA element of 601 *Cryphonectria parasitica*: ascospore inheritance and implications for mitochondrial recombination. *Mol. Gen. Genet.* 602 256:566-571. 603
39. Barr CM, Neiman M, Taylor DR. 2005. Inheritance and recombination of mitochondrial genomes in plants, fungi 604 and animals. *New Phytol.* 168:39-50. 605
40. Peterson A, Jacobsen S-E, Bonifacio A, Murphy K. 2015. A Crossing Method for Quinoa. *Sustainability* 7:3230-606 3243. 607
41. Boccardo G, Lisa V, Luisoni E, Milne RG. 1987. Cryptic plant viruses, p 171-214, *Adv Virus Res*, vol 32. 608 Elsevier. 609
42. Natsuaki T, Yamashita S, Doi Y, Yora K. 1979. Radish Yellow Edge Virus, a seed-borne small spherical virus 610 newly recognized in Japanese radish (*Raphanus sativus* L.). *Ann Phyt Soc Jap* 45:313-320. 611
43. Kassanis B, White RF, Woods RD. 1977. Beet cryptic virus. *J Phytopathol* 90:350-360. 612
44. Boccardo G, Milne RG, Luisoni E, Lisa V, Accotto GP. 1985. Three seedborne cryptic viruses containing double-613 stranded RNA isolated from white clover. *Virology* 147:29-40. 614
45. Chen S, Cao L, Huang Q, Qian Y, Zhou X. 2016. The complete genome sequence of a novel maize-associated 615 totivirus. *Arch Virol* 161:487-490. 616
46. Liu HQ, Fu YP, Xie JT, Cheng JS, Ghabrial SA, Li GQ, Peng YL, Yi XH, Jiang DH. 2012. Evolutionary 617 genomics of mycovirus-related dsRNA viruses reveals cross-family horizontal gene transfer and evolution of diverse viral 618 lineages. *BMC Evol Biol* 12:91. 619
47. Covelli L, Coutts RHA, Di Serio F, Citir A, Acikgoz S, Hernandez C, Ragozzino A, Flores R. 2004. Cherry 620 chlorotic rusty spot and Amasya cherry diseases are associated with a complex pattern of mycoviral-like double-stranded 621 RNAs. I. Characterization of a new species in the genus *Chrysovirus*. *J Gen Virol* 85:3389-3397. 622
48. Li LQ, Liu JN, Xu AX, Wang T, Chen JS, Zhu XW. 2013. Molecular characterization of a trisegmented 623 chrysovirus isolated from the radish *Raphanus sativus*. *Virus Res* 176:169-178. 624
49. Safari M, Roossinck MJ. 2018. Coevolution of a Persistent Plant Virus and Its Pepper Hosts. *Mol Plant Microbe* 625 *Interact* 31:766-776. 626
50. Liu W, Chen J. 2009. A double-stranded RNA as the genome of a potential virus infecting *Vicia faba*. *Virus* 627 *Genes* 39:126-131. 628
51. Martin RR, Zhou J, Tzanetakis IE. 2011. Blueberry latent virus: An amalgam of the Partitiviridae and Totiviridae. 629 *Virus Res* 155:175-180. 630
52. Sabanadzovic S, Valverde RA, Brown JK, Martin RR, Tzanetakis IE. 2009. Southern tomato virus: The link 631 between the families Totiviridae and Partitiviridae. *Virus Res* 140:130-137. 632
53. Salem NM, Golino DA, Falk BW, Rowhani A. 2008. Complete nucleotide sequences and genome 633 characterization of a novel double-stranded RNA virus infecting *Rosa multiflora*. *Arch Virol* 153:455-462. 634
54. Roossinck MJ. 2015. Metagenomics of plant and fungal viruses reveals an abundance of persistent lifestyles. 635 *Front Microbiol* 5:767. 636
55. Roossinck MJ. 2012. Persistent plant viruses: molecular hitchhikers or epigenetic elements?, p 177-186, *Viruses: 637 Essential Agents of Life*. Springer. 638
56. Roossinck MJ. 2017. Deep sequencing for discovery and evolutionary analysis of plant viruses. *Virus Res* 639 239:82-86. 640

on February 4, 2019 by guest<http://jvi.asm.org/>Downloaded from

57. Valverde RA, Gutierrez DL. 2008. Molecular and biological properties of a putative partitivirus from jalapeño 641
pepper (*Capsicum annuum* L.). *Rev Mex Fitopatol* 26:1-6. 642
58. Pantaleo V, Vitali M, Boccacci P, Miozzi L, Cuzzo D, Chitarra W, Mannini F, Lovisolo C, Gambino G. 2016. 643
Novel functional microRNAs from virus-free and infected *Vitis vinifera* plants under water stress. *Sci Rep* 6:20167. 644
59. Perrone I, Chitarra W, Boccacci P, Gambino G. 2017. Grapevine-virus-environment interactions: an intriguing 645
puzzle to solve. *New Phytol* 213:983-987. 646
60. Jacoby RP, Li L, Huang S, Pong Lee C, Millar AH, Taylor NL. 2012. Mitochondrial Composition, Function and 647
Stress Response in Plants. *J Integr Plant Biol* 54:887-906. 648
61. Nerva L, Ciuffo M, Vallino M, Margaria P, Varese GC, Gnani G, Turina M. 2016. Multiple approaches for the 649
detection and characterization of viral and plasmid symbionts from a collection of marine fungi. *Virus Res.* 219:22-38. 650
62. Dhir A, Dhir S, Borowski LS, Jimenez L, Teitell M, Rotig A, Crow YJ, Rice GI, Duffy D, Tamby C, Nojima T, 651
Munnich A, Schiff M, de Almeida CR, Rehwinkel J, Dziembowski A, Szczesny RJ, Proudfoot NJ. 2018. Mitochondrial 652
double-stranded RNA triggers antiviral signalling in humans. *Nature* 560:238-242. 653
63. Wang M-B, Masuta C, Smith NA, Shimura H. 2012. RNA Silencing and Plant Viral Diseases. *Mol Plant Microbe* 654
Interact 25:1275-1285. 655
64. Ruwe H, Wang GW, Gusewski S, Schmitz-Linneweber C. 2016. Systematic analysis of plant mitochondrial and 656
chloroplast small RNAs suggests organelle-specific mRNA stabilization mechanisms. *Nucleic Acids Res* 44:7406-7417. 657
65. Barkan A, Small I. 2014. Pentatricopeptide Repeat Proteins in Plants. *Annu Rev Plant Biol* 65:415-442. 658
66. Krishnamurthy SR, Janowski AB, Zhao G, Barouch D, Wang D. 2016. Hyperexpansion of RNA Bacteriophage 659
Diversity. *PLOS Biol* 14:e1002409. 660
67. Krishnamurthy SR, Wang D. 2018. Extensive conservation of prokaryotic ribosomal binding sites in known and 661
novel picobirnaviruses. *Virology* 516:108-114. 662
68. Doron S, Melamed S, Ofir G, Leavitt A, Lopatina A, Keren M, Amitai G, Sorek R. 2018. Systematic discovery of 663
antiphage defense systems in the microbial pangenome. *Science* 359:6379. 664
69. Hale CR, Zhao P, Olson S, Duff MO, Graveley BR, Wells L, Terns RM, Terns MP. 2009. RNA-Guided RNA 665
Cleavage by a CRISPR RNA-Cas Protein Complex. *Cell* 139:945-956. 666
70. Marraffini LA, Sontheimer EJ. 2010. CRISPR interference: RNA-directed adaptive immunity in bacteria and 667
archaea. *Nat Rev Genet* 11:181-190. 668
71. Marraffini LA. 2015. CRISPR-Cas immunity in prokaryotes. *Nature* 526:55-61. 669
72. Tamulaitis G, Kazlauskienė M, Manakova E, Venclovas C, Nwokeoji AO, Dickman MJ, Horvath P, Siksnys V. 670
2014. Programmable RNA Shredding by the Type III-A CRISPR-Cas System of *Streptococcus thermophilus*. *Mol Cell* 671
56:506-517. 672
73. Haas BJ, Papanicolaou A, Yassour M, Grabherr M, Blood PD, Bowden J, Couger MB, Eccles D, Li B, Lieber M. 673
2013. De novo transcript sequence reconstruction from RNA-seq using the Trinity platform for reference generation and 674
analysis. *Nat Protoc* 8:1494-1512. 675
74. Altschul SF, Madden TL, Schaffer AA, Zhang JH, Zhang Z, Miller W, Lipman DJ. 1997. Gapped BLAST and 676
PSI-BLAST: a new generation of protein database search programs. *Nucleic Acids Res* 25:3389-3402. 677
75. Li H, Durbin R. 2009. Fast and accurate short read alignment with Burrows-Wheeler transform. *Bioinformatics* 678
25:1754-1760. 679
76. Li H, Handsaker B, Wysoker A, Fennell T, Ruan J, Homer N, Marth G, Abecasis G, Durbin R, Genome Project 680
Data P. 2009. The Sequence Alignment/Map format and SAMtools. *Bioinformatics* 25:2078-2079. 681
77. Turina M, Prodi A, Van Alfen NK. 2003. Role of the Mf1-1 pheromone precursor gene of the filamentous 682
ascomycete *Cryphonectria parasitica*. *Fungal Genet Biol* 40:242-251. 683
78. Gruber AR, Lorenz R, Bernhart SH, Neuböck R, Hofacker IL. 2008. The vienna RNA websuite. *Nucleic Acids* 684
Res 36:W70-W74. 685
79. Huson DH, Beier S, Flade I, Gorska A, El-Hadidi M, Mitra S, Ruscheweyh HJ, Tappu R. 2016. MEGAN 686
Community Edition - Interactive Exploration and Analysis of Large-Scale Microbiome Sequencing Data. *PLoS Comput* 687
Biol 12: e1004957. 688
80. Zerbino DR, Birney E. 2008. Velvet: algorithms for de novo short read assembly using de Bruijn graphs. *Genome* 689
Res 18:821-829. 690
81. Schulz MH, Zerbino DR, Vingron M, Birney E. 2012. Oases: robust de novo RNA-seq assembly across the 691
dynamic range of expression levels. *Bioinformatics* 28:1086-1092. 692
82. Afgan E, Baker D, Batut B, van den Beek M, Bouvier D, Cech M, Chilton J, Clements D, Coraor N, Gruening 693
BA, Guerler A, Hillman-Jackson J, Hiltmann S, Jalili V, Rasche H, Soranzo N, Goecks J, Taylor J, Nekrutenko A, 694
Blankenberg D. 2018. The Galaxy platform for accessible, reproducible and collaborative biomedical analyses: 2018 695
update. *Nuc. Acids Res.* 46:W537-W544. 696
83. Lawrence M, Huber W, Pages H, Aboyoun P, Carlson M, Gentleman R, Morgan MT, Carey VJ. 2013. Software 697
for Computing and Annotating Genomic Ranges. *PLoS Comput Biol* 9: e1003118. 698
84. Tamura K, Stecher G, Peterson D, Filipski A, Kumar S. 2013. MEGA6: Molecular Evolutionary Genetics 699
Analysis Version 6.0. *Mol Biol Evol* 30:2725-2729. 700
85. Dimmic MW, Rest JS, Mindell DP, Goldstein RA. 2002. rtREV: An amino acid substitution matrix for inference 701
of retrovirus and reverse transcriptase phylogeny. *J Mol Evol* 55:65-73. 702

86. Vigani G, Bohic S, Faoro F, Vekemans B, Vincze L, Terzano R. 2018. Cellular Fractionation and Nanoscopic X-703
Ray Fluorescence Imaging Analyses Reveal Changes of Zinc Distribution in Leaf Cells of Iron-Deficient Plants. *Front* 704
Plant Sci 9:1112. 705
87. Vigani G, Faoro F, Ferretti AM, Cantele F, Maffi D, Marelli M, Maver M, Murgia I, Zocchi G. 2015. Three-706
Dimensional Reconstruction, by TEM Tomography, of the Ultrastructural Modifications Occurring in *Cucumis sativus* L. 707
Mitochondria under Fe Deficiency. *PLoS One* 10:e0129141. 708
88. Nerva L, Varese GC, Falk BW, Turina M. 2017. Mycoviruses of an endophytic fungus can replicate in plant cells: 709
evolutionary implications. *Sci Rep* 7:1908-1908. 710
89. Perrotta G, Grienemberger JM, Gualberto JM. 2002. Plant mitochondrial rps2 genes code for proteins with a C-711
terminal extension that is processed. *Plant Mol Biol* 50:523-533. 712
90. Kim Y, Kim HD, Kim J. 2013. Cytoplasmic ribosomal protein S3 (rpS3) plays a pivotal role in mitochondrial 713
DNA damage surveillance. *Biochim Biophys Acta Mol Cell Res* 1833:2943-2952. 714
91. Suenkel S, Brennicke A, Knoop V. 1994. RNA editing of a conserved reading frame in plant mitochondria 715
increases its similarity to two overlapping reading frames in *Escherichia coli*. *Mol Gen Genet* 242:65-72. 716
92. Sambrook J, Fritsch EF, Maniatis T. 1989. *Molecular Cloning: A Laboratory Manual*, Ed 2. Cold Spring Harbor 717
Laboratory Press, Cold Spring Harbor, NY. 718
93. Moretti M, Ciuffo M, Gotta P, Prodorutti D, Bragagna P, Turina M. 2011. Molecular characterization of two 719
distinct strains of blueberry scorch virus (BIScV) in northern Italy. *Arch Virol* 156:1295-1297. 720
94. Margaria P, Rosa C, Marzachi C, Turina M, Palmano S. 2007. Detection of Flavescence doree phytoplasma in 721
grapevine by reverse-transcription PCR. *Plant Dis* 91:1496-1501. 722
723

FIGURE LEGENDS 724

- 725
FIG 1 *Chenopodium quinoa* mitovirus 1 (CqMV1) genome organization and its replicative nature. (A) genome 726
organization of the single positive strand genome with the RdRp ORF (blue box). The position of the two DNA segments 727
amplified by reverse transcriptase PCR and used as probes in northern hybridization experiments are shown as black lines 728
(Probe 1 and Probe 2). nt= nucleotide position on the genome. (B) Ethidium bromide stained TAE gel (1%) to separate 729
PCR products from RNA template and DNA template extracted from *Chenopodium quinoa* IPSP1. M= molecular weight 730
marker; RT= reverse transcriptase; no-RT= RNA template without reverse transcriptase. Kb=kilobases. 731
732
- FIG 2 *Chenopodium quinoa* mitovirus 1 phylogenetic placement. Predicted ORF encoding RdRp were used to build an 733
alignment using MUSCLE implemented in MEGA 6 (Tamura et al. 2013). Phylogenetic tree was built using the maximum 734
likelihood method with 1000 bootstrap replicates. Branches with bootstrap value <50 have been collapsed. The analysis 735
involved 125 amino acid sequences. All positions with less than 90% site coverage were eliminated. There were a total of 736
457 positions in the final dataset. A list of the accession numbers of the viruses contained in the tree is shown in 737
supplementary on line Table 2. The diamond symbol represents a node that was collapsed, which includes 27 RdRp 738
sequences from a number of invertebrate and plant ourmiaviruses, still awaiting a taxonomical classification. Asterisks 739
indicate endogenized plant mitochondrial sequences. 740
741
- FIG 3 *Chenopodium quinoa* mitovirus 1 (CqMV1) genomic RNA is enriched in mitochondrial fractions. (A) Fluorescent 742
microscopy observation of mitochondria (a-c) and chloroplasts (d-f) fractions purified from *Chenopodium quinoa* leaves. 743
a, d: bright-field; b, e: chlorophyll fluorescence; c, f: overlay of the two images. Magnification bar: 50 μ m. (B) Real time 744
quantification of RNA corresponding to CqMV1 and two nuclear (Cox and S2) and two mitochondrial genes (OrfX and 745
S3). All quantifications are relative to the amount of virus or mRNA present in the Supernatant of the 14K centrifuge run: 746
such amount was arbitrarily established as 1. Error bars represent standard error of the mean (n=3). 747
748
- FIG 4 Evidence of minus strand genomic RNA accumulation. Time of autoradiography exposure is indicated at the 749
bottom of each panel (exp); RNA samples were extracted from leaves from uninfected *Chenopodium quinoa* accession 750
BO25 (V-) and from *Chenopodium quinoa* mitovirus 1 (CqMV1)-infected *Chenopodium quinoa* cultivar Regalona (V+). 751
In each panel, negative sense probe reacting with the viral positive RNA strand is shown on the left and positive strand 752
probe reacting with the viral negative RNA strand is shown on the right. Asterisks show weak specific signals given by 753
positive probes targeting the viral negative RNA strand. (A) panel shows signal from the two orientations of Probe 1 (see 754
Fig. 1), (B) panel shows signal given by Probe 2 (see Fig. 1). Lower panels are methylene blue stained membranes 755
showing ribosomal RNAs loading (rRNA). 756
757

FIG 5 Differential symptom severity of virus infections: local symptoms in leaves. Two *Chenopodium quinoa* mitovirus 1 (CqMV1) infected accessions (cv Regalona and IPSP1) and two CqMV1-free accessions (BO25 and BO75) were used to assess their responses when inoculated with pathogenic viruses. Observations were done at 7 days post inoculation (dpi). In panel A, alfalfa mosaic virus (AMV) locally inoculated leaves did not show differences in term of symptoms severity between CqMV1-infected and CqMV1-free accessions. In panel B, infection with Lettuce mosaic virus (LMV) revealed differences between CqMV1-infected accessions, in which chlorotic lesions were observed, and CqMV1-free accessions, in which necrotic lesion (red arrows) were observed. In panel C, infection with Hibiscus latent ringspot virus (HLRSV) did not revealed symptom differences among the four accessions.

FIG 6 Differential symptom severity of virus infections: systemic symptoms. Two *Chenopodium quinoa* mitovirus 1 (CqMV1) infected accessions and two CqMV1-free accessions were used to assess their responses when inoculated with three pathogenic viruses. Observations were done at 14 days post inoculation. In vertical rows the virus species used in the experiments: alfalfa mosaic virus (AMV) A,D,G,J; Lettuce mosaic virus (LMV) B,E,H,K; Hibiscus latent ring spot virus (HLRSV) C,F,I,L. In horizontal rows the four *Chenopodium quinoa* accessions BO78, BO25, IPSP1, and Regalona (Regal.) are reported. A negative mock-inoculated plant of the same age is present next to two infected plants in each panel. All accessions shows systemic symptoms of mild growth impairment, malformation and mild mottling. CqMV1-free accessions BO78 (A,B,C) and BO25 (D,E,F), showed red-violet pigmentation on stems (white arrows) whereas CqMV1 infected accessions IPSP1 (G,H,I) and Regalona (J,K,L) and mock inoculated plants did not showed any pigmentation. Inset of a pigmented stem from accession BO78 infected by LMV (panel B) is enlarged in panel M, whereas inset of a stem of cultivar Regalona also infected by LMV (panel K) is enlarged in panel N.

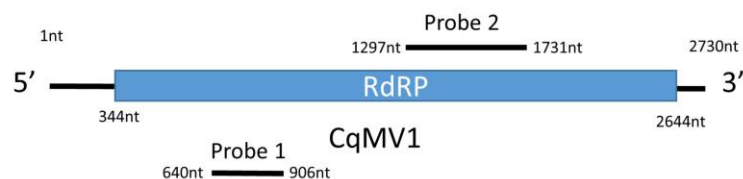
FIG 7 Small RNA (sRNA) length distribution in virus infected *Chenopodium quinoa* leaves. Reads from small RNA sequencing were mapped against genes encoded by chloroplast, nucleus, mitochondrion, alfalfa mosaic virus (AMV) and *Chenopodium quinoa* mitovirus 1 (CqMV1) genomes. Abundance is expressed as percentage of reads of a particular length and arrows above bars indicates the most abundant sRNA length inside the specific gene set. CqMV1 shared the same sRNA pattern distribution of genes encoded by the mitochondrial genomes, suggesting a mitochondrial localization and a specific but still uncharacterized RNA-degradation pathway inside the mitochondria.

on February 4, 2019 by guest<http://jvi.asm.org/>Downloaded from
Table 1. Small RNA reads mapping against each of the corresponding genomes as a percentage of total reads in *Chenopodium quinoa* cv Regalona, cv. Regalona infected with AMV and BO78 infected with AMV.

Table 1. Small RNA reads mapping against each of the corresponding genomes as a percentage of total reads in *Chenopodium quinoa* cv Regalona, cv. Regalona infected with AMV and BO78 infected with AMV.

	Chloroplast	CqMV1	Nucleus	AMV	Mitochondria	Total
Regalona	14.017	0.006	84.071	0.000	1.906	4119721
Regalona AMV	14.783	0.111	78.580	4.583	1.945	7240581
BO78 AMV	15.262	0.000	80.333	2.489	1.916	3758683

A



B

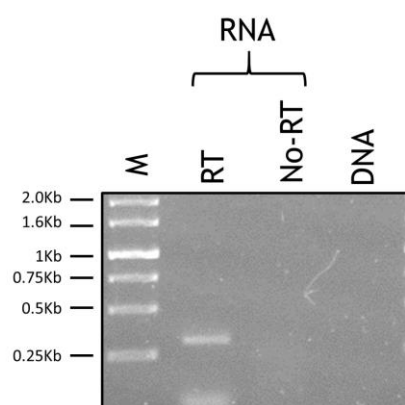


FIG 1 *Chenopodium quinoa* mitovirus 1 (CqMV1) genome organization and its replicative nature. (A) genome organization of the single positive strand genome with the RdRp ORF (blue box). The position of the two DNA segments amplified by reverse transcriptase PCR and used as probes in northern hybridization experiments are shown as black lines (Probe 1 and Probe 2). nt= nucleotide position on the genome. (B) Ethidium bromide stained TAE gel (1%) to separate PCR products from RNA template and DNA template extracted from *Chenopodium quinoa* IPSP1. M= molecular weight marker; RT= reverse transcriptase; no-RT= RNA template without reverse transcriptase. Kb=kilobases.

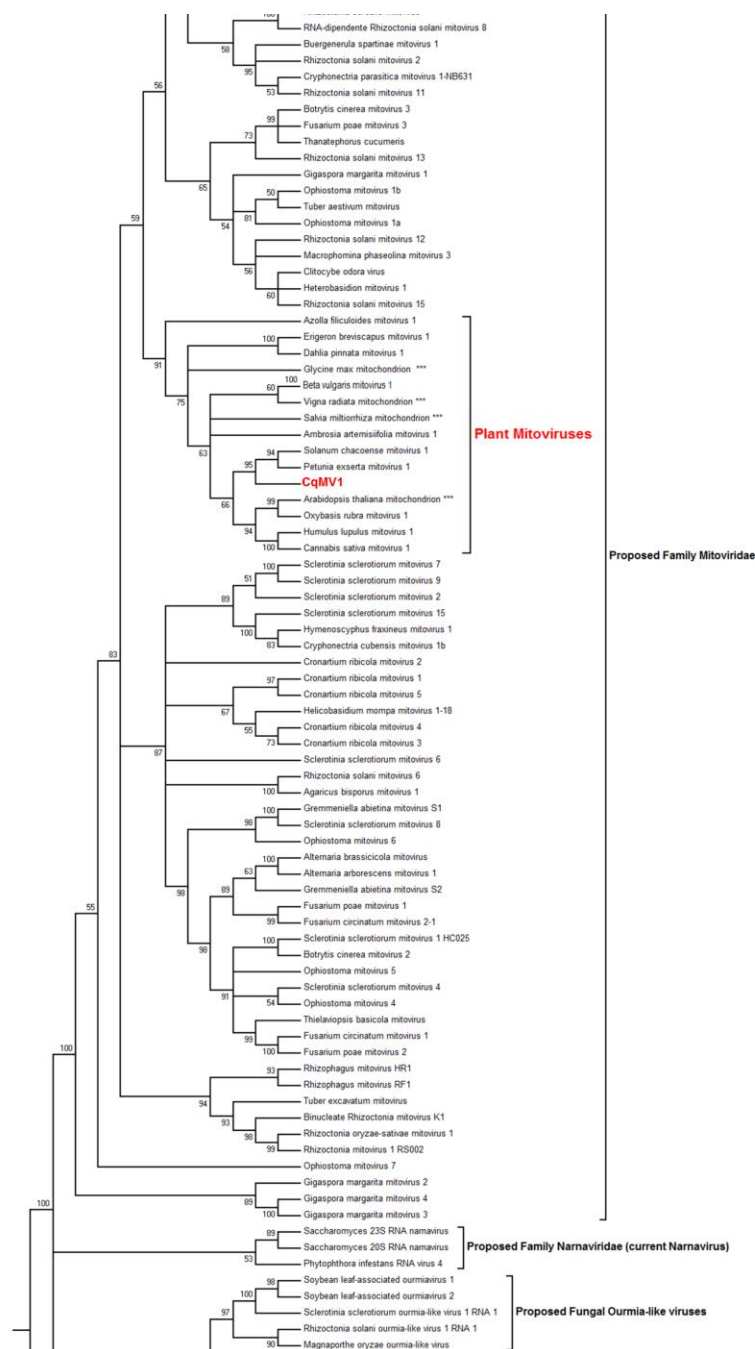


FIG 2 *Chenopodium quinoa* mitovirus 1 phylogenetic placement. Predicted ORF encoding RdRp were used to build an 733 alignment using MUSCLE implemented in MEGA 6 (Tamura et al. 2013). Phylogenetic tree was built using the maximum 734 likelihood method with 1000 bootstrap replicates. Branches with bootstrap value <50 have been collapsed. The analysis 735 involved 125 amino acid sequences. All positions with less than 90% site coverage were eliminated. There were a total of 736 457 positions in the final dataset. A list of the accession numbers of the viruses contained in the tree is shown in 737 supplementary on line Table 2. The diamond symbol represents a node that was collapsed, which includes 27 RdRp 738 sequences from a number of invertebrate and plant ourmiaviruses, still awaiting a taxonomical classification. Asterisks 739 indicate endogenized plant mitochondrial sequences.

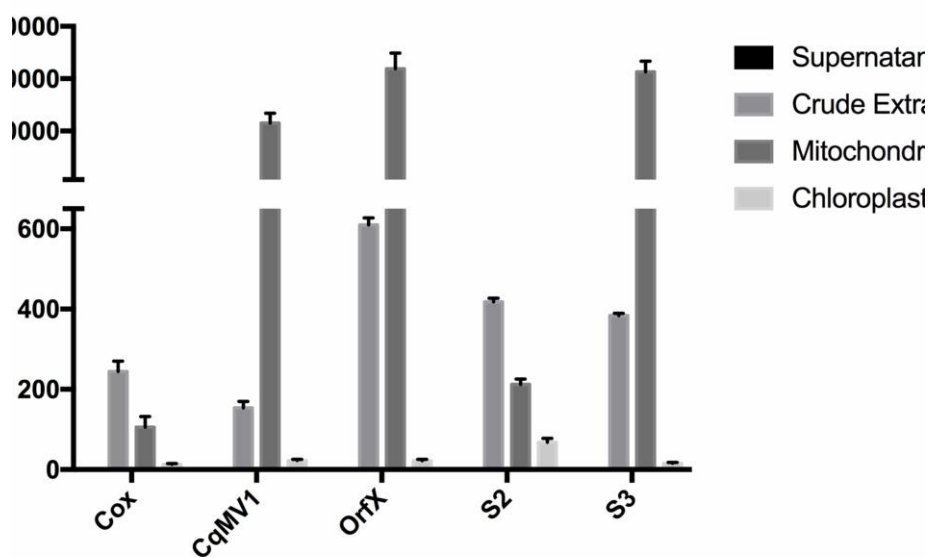
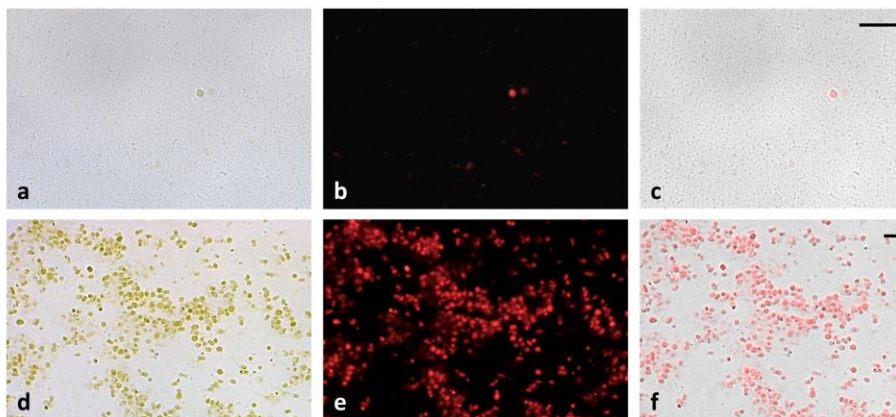


FIG 3 *Chenopodium quinoa* mitovirus 1 (CqMV1) genomic RNA is enriched in mitochondrial fractions. (A) Fluorescent 742 microscopy observation of mitochondria (a-c) and chloroplasts (d-f) fractions purified from *Chenopodium quinoa* leaves. 743 a, d: bright-field; b, e: chlorophyll fluorescence; c, f: overlay of the two images. Magnification bar: 50 μ m. (B) Real time 744 quantification of RNA corresponding to CqMV1 and two nuclear (Cox and S2) and two mitochondrial genes (OrfX and 745 S3). All quantifications are relative to the amount of virus or mRNA present in the Supernatant of the 14K centrifuge run: 746 such amount was arbitrarily established as 1. Error bars represent standard error of the mean (n=3).

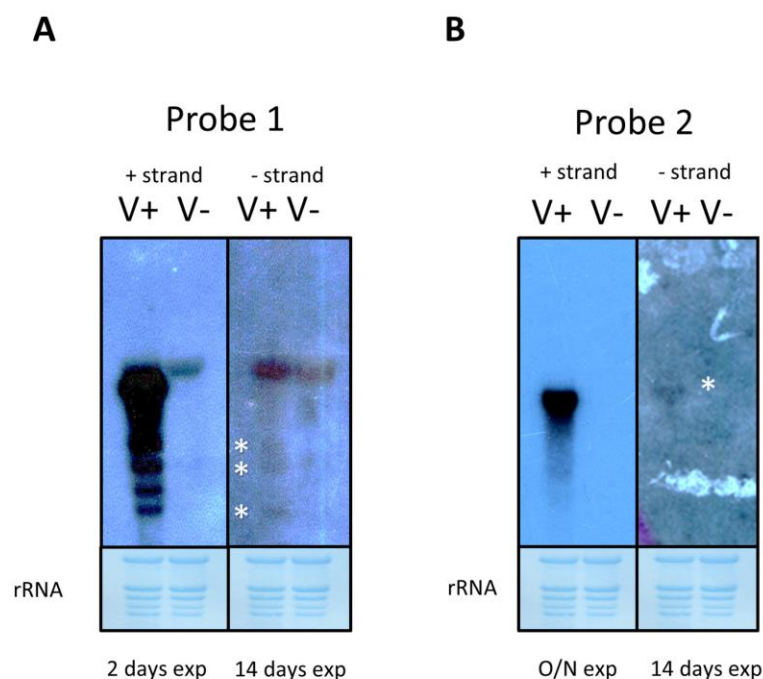


FIG 4 Evidence of minus strand genomic RNA accumulation. Time of autoradiography exposure is indicated at the bottom of each panel (exp); RNA samples were extracted from leaves from uninfected *Chenopodium quinoa* accession BO25 (V-) and from *Chenopodium quinoa* mitovirus 1 (CqMV1)-infected *Chenopodium quinoa* cultivar Regalona (V+). In each panel, negative sense probe reacting with the viral positive RNA strand is shown on the left and positive sense probe reacting with the viral negative RNA strand is shown on the right. Asterisks show weak specific signals given by positive probes targeting the viral negative RNA strand. (A) panel shows signal from the two orientations of Probe 1 (see Fig. 1), (B) panel shows signal given by Probe 2 (see Fig. 1). Lower panels are methylene blue stained membranes showing ribosomal RNAs loading (rRNA).

Fig. 5

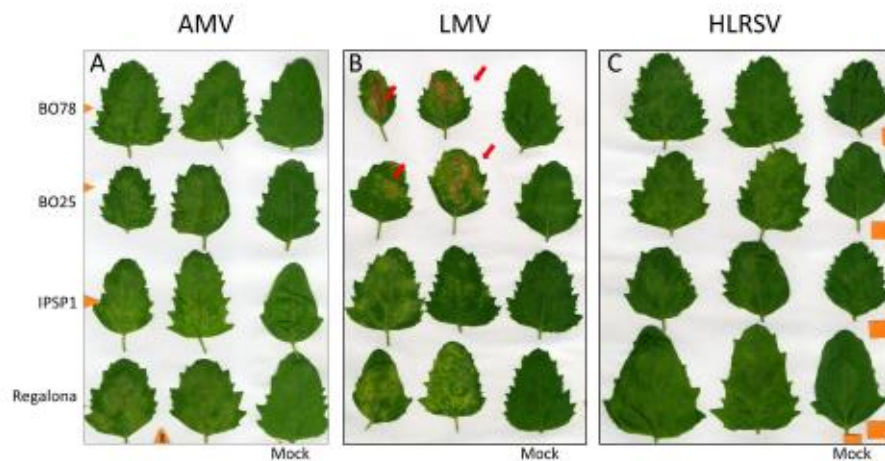


FIG 5 Differential symptom severity of virus infections: local symptoms in leaves. Two *Chenopodium quinoa* mitovirus 1 758 (CqMV1) infected accessions (cv Regalona and IPSP1) and two CqMV1-free accessions (BO25 and BO75) were used to 759 assess their responses when inoculated with pathogenic viruses. Observations were done at 7 days post inoculation (dpi). 760 In panel A, alfalfa mosaic virus (AMV) locally inoculated leaves did not show differences in term of symptoms severity 761 between CqMV1-infected and CqMV1-free accessions. In panel B, infection with Lettuce mosaic virus (LMV) revealed 762 differences between CqMV1-infected accessions, in which chlorotic lesions were observed, and CqMV1-free accessions, 763 in which necrotic lesion (red arrows) were observed. In panel C, infection with Hibiscus latent ringspot virus (HLRSV) did 764 not revealed symptom differences among the four accessions

Figure 6

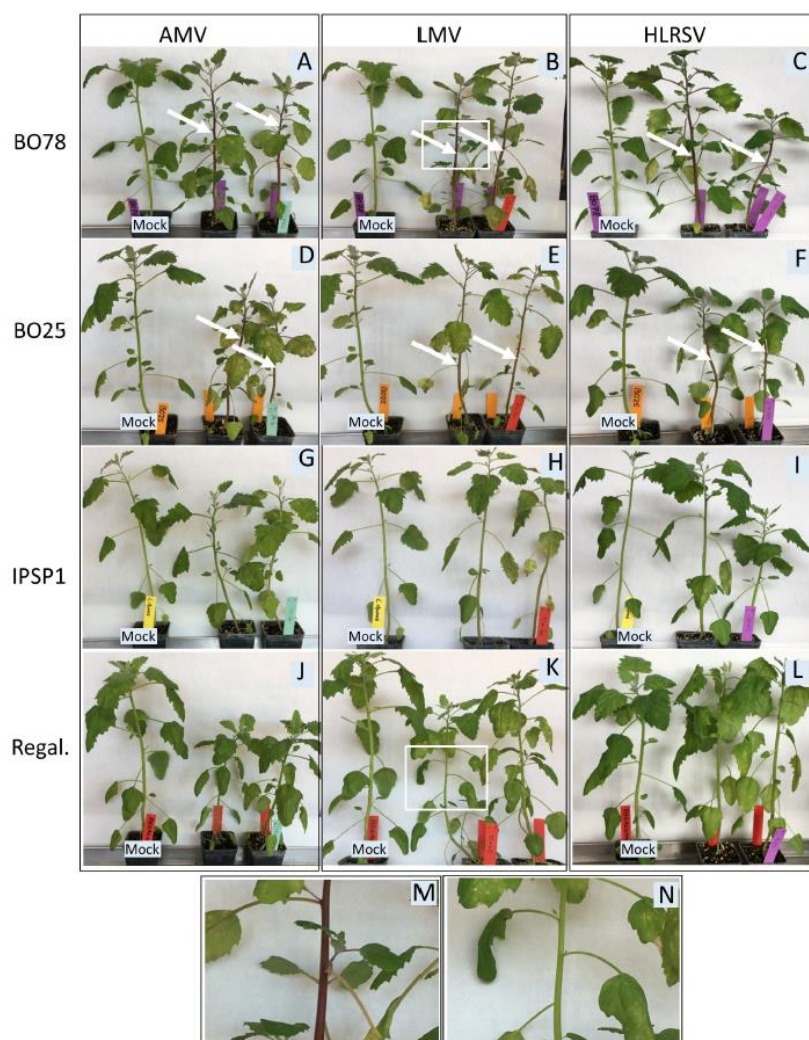


FIG 6 Differential symptom severity of virus infections: systemic symptoms. Two *Chenopodium quinoa* mitovirus 1 767 (CqMV1) infected accessions and two CqMV1-free accessions were used to assess their responses when inoculated with 768 three pathogenic viruses. Observations were done at 14 days post inoculation. In vertical rows the virus species used in the 769 experiments: alfalfa mosaic virus (AMV) A,D,G,J; Lettuce mosaic virus (LMV) B,E,H,K; Hibiscus latent ring spot virus 770 (HLRSV) C,F,I,L. In horizontal rows the four *Chenopodium quinoa* accessions BO78, BO25, IPSP1, and Ragalona 771 (Regal.) are reported. A negative mock-inoculated plant of the same age is present next to two infected plants in each 772 panel. All accessions shows systemic symptoms of mild growth impairment, malformation and mild mottling. CqMV1-773 free accessions BO78 (A,B,C) and BO25 (D,E,F), showed red-violet pigmentation on stems (white arrows) whereas 774 CqMV1 infected accessions IPSP1 (G,H,I) and Regalona (J,K,L) and mock inoculated plants did not showed any 775 pigmentation. Inset of a pigmented stem from accession BO78 infected by LMV (panel B) is enlarged in panel M, whereas 776 inset of a stem of cultivar Regalona also infected by LMV (panel K) is enlarged in panel N.

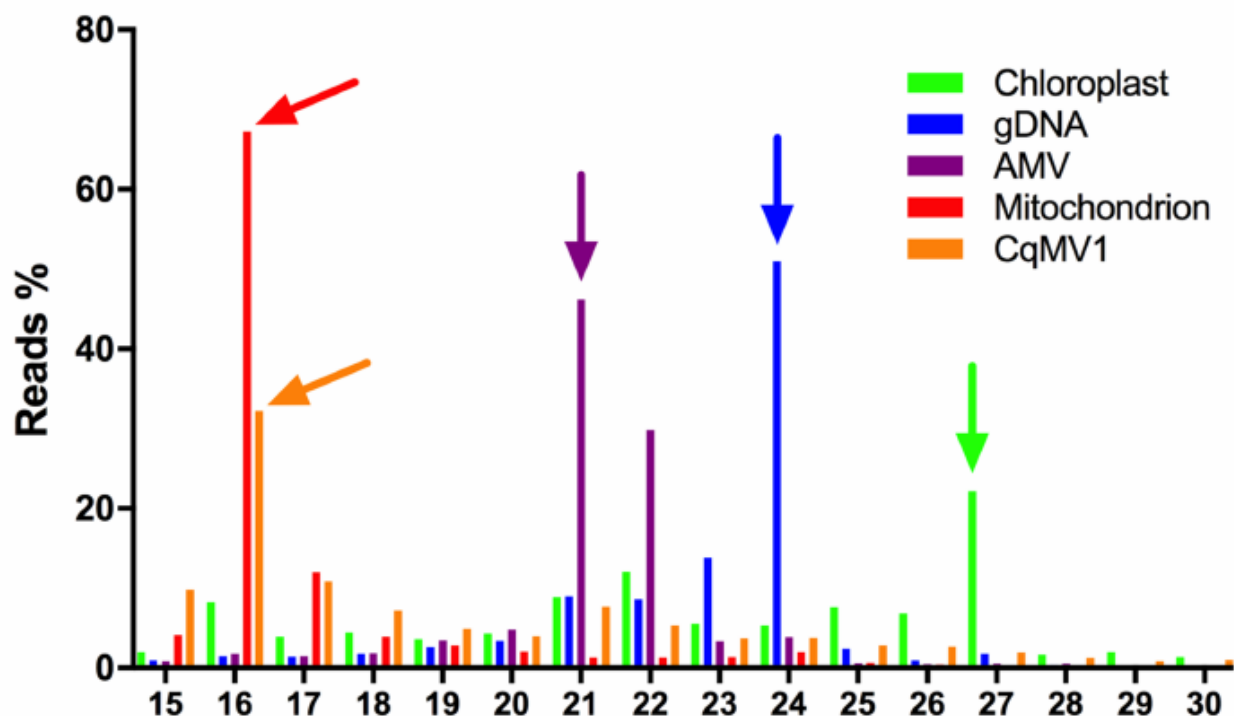


FIG 7 Small RNA (sRNA) length distribution in virus infected *Chenopodium quinoa* leaves. Reads from small RNA 779 (sRNA) sequencing were mapped against genes encoded by chloroplast, nucleus, mitochondrion, alfalfa mosaic virus 780 (AMV) and *Chenopodium quinoa* mitovirus 1 (CqMV1) genomes. Abundance is expressed as percentage of reads of a 781 particular length and arrows above bars indicates the most abundant sRNA length inside the specific gene set. CqMV1 782 shared the same sRNA pattern distribution of genes encoded by the mitochondrial genomes, suggesting a mitochondrial 783 localization and a specific but still uncharacterized RNA-degradation pathway inside the mitochondria.